Pergamon

CEMENT AND CONCRETE RESEARCH

Cement and Concrete Research 33 (2003) 489–497

The hydration phase and pore structure formation in the blends of sulfoaluminate-belite cement with Portland cement

I. Janotka[a,*], L’. Krajči[a], A. Ray[b], S.C. Mojumdar[c]

[a]*Institute of Construction and Architecture, Slovak Academy of Sciences, Dúbravská cesta 9, 842 20 Bratislava, Slovakia*
[b]*Department of Materials Science, University of Technology, Sydney, P.O. Box 123, Broadway, Sydney, NSW, 2007, Australia*
[c]*Institute of Inorganic Chemistry, Slovak Academy of Sciences, Dúbravská cesta 9, 842 36 Bratislava, Slovakia*

Received 25 July 2001; accepted 11 September 2002

Abstract

Sulfoaluminate-belite (SAB) cements are an attractive class of low-energy cements from the viewpoint of saving energy and releasing less CO_2 into the atmosphere during their production. Their hydraulic activity, however, does not match that of the ordinary Portland cement (PC) and needs improvement before they can be used on their own. However, SAB cements when blended with PC have the potential to be used effectively in traditional applications as shown by this study. Mortars made with blends of SAB cements and PC, and a cement-to-sand ratio of 1:3 by weight and a water-to-cement ratio of 0.5, indicate a superior protection against corrosion of steel to those made with blends of PC and blast-furnace slag (BFSPC). The prepared mortars were stored at 20 °C for 90 days under either a 60% relative humidity (RH)–dry air, or 100% RH–wet air conditions. With further improvement in the SAB cement quality through better understanding of their characteristics, a genuine competition between SAB/PC and BFSPC can be expected in practice.

© 2002 Elsevier Science Ltd. All rights reserved.

Keywords: Hydration; X-ray diffraction; Corrosion; Blended cement; Mortar

1. Introduction

The manufacture of Portland cement (PC) consumes not only a vast amount of energy but it also generates undesirable CO_2 emissions. Much attention in recent years has been given to the development of a new generation of cements with the aim of saving energy [1]. To this end, blended cements have been successfully developed by the concrete industry. Nevertheless, in order for the blended cements to play a greater role, they must be incorporated into more products, must be able to provide improved engineering properties and must be capable of offering improved resistance to chemical attack, freeze–thaw and alkali–aggregate reactions [2–4]. One such cement containing the main phases C_2S, $C_4A_3\bar{S}$, C_4AF and $C\bar{S}$ has been developed and reported by many researchers [5–10]. This special cement contains calcium sulfoaluminate instead of high-temperature and hence high-energy tricalcium silicate and tricalcium aluminate. Raw mixes for $C_4A_3\bar{S}$ clinkers differ from those for PC in that they contain significant amounts of sulfates; therefore, the reactions and products are different from those found in PC production [11–14]. Calcium sulfoaluminate-based cement compositions containing more than 50% $C_4A_3\bar{S}$ show expansion, cracking and loss of strength at later ages [15]. Compositions with more than 20% $C_4A_3\bar{S}$ gave progressively lower mechanical strength, when hydrated with the fixed water/reactants ($C_4A_3\bar{S}+C\bar{S}$) ratio of 0.86. The best properties were obtained with cements containing 30–40% $C_4A_3\bar{S}$ at water-to-cement ratio about 0.35 to 0.50 [15]. Cements containing $C_4A_3\bar{S}$, β-C_2S and $C\bar{S}$ at 1.5:1:1 weight ratio hydrate rapidly to ettringite and develop early strength. All these compositions have very good dimensional stabilities, similar to PC and good resistance to atmospheric carbonation, although the ettringite component in hydrated cement tends to carbonate [16–18]. Preliminary results show that resistance of sulfoaluminate-based cements to hydrochloric acid, sodium sulfate and sodium chloride solutions is very similar to that of PC [19], but their resistance to freezing and thawing is considerably lower [20]. Macro-defect free (MDF) materials based on sulfoaluminate-belite (SAB) clinkers were synthesized and showed sufficient moisture resistance due to organic phase occurrence [21,22]. An experimental study on the upgrade of

---

[*] Corresponding author. Tel.: +421-2-5941-2298; fax: +421-2-5477-2494.

E-mail address: usarivan@savba.sk (I. Janotka).

0008-8846/02/$ – see front matter © 2002 Elsevier Science Ltd. All rights reserved.
PII: S0008-8846(02)00994-8

SAB cement systems by blending with PC indicated an increase in strength and dynamic modulus of elasticity as well as the decreased water absorption capacity of the blend compared with SAB cement. Passivation of steel in a blend of 85 wt.% SAB cement with 15 wt.% of PC is comparable to that in the pure PC system [23].

The present paper is concerned with the effect of SAB cement and its blends on the mechanical properties of mortar specimens, the development of hydrate phases and pore structure as well as the ability of mortars to protect steel against corrosion. The results obtained with pure SAB cements and their blends with PC are compared with those of PC and blast-furnace slag Portland cement (BFSPC).

2. Experimental

2.1. Materials

PC CEM I 42.5, BFSPC with 30 wt.% of blast-furnace slag, and two types of SAB (SAB 1 and SAB 2) cements were used in the tests. The SAB cements were mixed with PC in the weight ratio of 85% to 15% and basic characteristics of the cements are listed in Tables 1 and 2. Four cements (PC, BFSPC, SAB 1 and SAB 2) and two mixed cements were used to prepare mortar specimens with cement-to-sand proportion of 1:3 (40 × 40160 mm) and water/cement ratio of 0.5. Siliceous sand in fractions of 0–0.5, 0.5–1.0 and 1.0–2.0 mm in weight ratio of 1:1:1 was used. The SAB cement samples were synthesized at the Slovak Technical University, Bratislava, Department of Ceramics, Glass and Cement. The cements differed in their raw mix composition. The firing temperature was 1250 °C.

2.2. Test methodologies

The specimens were stored at 20 °C and 100% RH for 7 days and subsequently at 20 °C/100% RH and at 20 °C/60% RH, respectively, for 83 days.

Table 2
Mineralogical composition of test cements

Type of the cement	Portion of clinker minerals (%)					
	C_3S	C_2S	C_3A	C_4AF	$C_4A_3\bar{S}$	$C\bar{S}$
PC (Bogue)	67.6	5.1	9.2	10.6	none	5.9
BFSPC	no calculation was done					
SAB 1	none	67.1	none	19.0	6.7	7.0
SAB 1/PC	10.1	57.8	1.4	17.7	5.7	6.8
SAB 2	none	59.7	none	19.6	5.8	7.1
SAB 2/PC	10.1	51.5	1.4	18.3	4.9	6.9

Mortar specimens were tested for compressive strength, water absorption capacity, specific gravity, volume density and total porosity. Water absorption capacity was determined from the decrease in weight of the specimens saturated by water and then dried at 105 °C to constant weight. The results are expressed in weight percent (wt.%). Total porosity was calculated from the volume density and specific gravity values using the formula:

$$\mathrm{TP} = \left(1 - \frac{\rho_{\mathrm{VD}}}{\rho_{\mathrm{SG}}}\right) \times 100 \tag{1}$$

where TP is the total porosity as the content of pores and voids in the specimens (%), ρ_{VD} is the volume density (kg m^{-3}) and ρ_{SG} is the specific gravity (kg m^{-3}). The volume density was estimated on the specimens of regular shape by weighing at calculated volume of the prisms. The specific gravity was ascertained by a pycnometric method as the weight of the volume unit of solid constituents of the mortar specimen in powdered stage.

Ultrasonic pulse velocities were measured on an ultrasonic apparatus (UNIPAN type 543, Poland) calculating the dynamic modulus of elasticity (E_{bu}) by the formula

$$E_{\mathrm{bu}} = \rho_{\mathrm{VD}}\gamma_{\mathrm{L}}^{2}10^{-6} \tag{2}$$

where E_{bu} is the dynamic modulus of elasticity (MPa), ρ_{VD} is the volume density (kg m^{-3}) and γ_{L} is the impulse speed of longitudinal ultrasonic waves (m s^{-1}).

Table 1
Chemical composition and basic properties of the cements

Chemical composition (wt.%)	Cements employed					
	PC	BFSPC	SAB 1	SAB 1/PC	SAB 2	SAB 2/PC
Humidity	0.02	0.24	0.35	0.02	0.04	0.03
Ignition loss	1.40	1.02	0.60	0.46	0.13	0.40
Ins. residue	1.66	1.51	0.16	0.57	4.60	3.94
SiO_2	19.51	24.88	23.46	22.62	20.87	21.09
CaO	63.60	55.18	55.06	58.50	54.59	55.41
MgO	1.49	4.70	1.78	0.46	1.38	1.78
Fe_2O_3	3.48	4.70	6.25	5.45	6.46	5.69
Al_2O_3	5.67	4.27	7.35	7.27	7.03	7.06
SO_3	3.01	3.22	4.99	4.65	4.90	4.60
CaO free	0.10	0	0.02	0.02	0.05	0.04
Specific gravity (kg m^{-3})	3168	3047	3236	3152	3234	3166
Surface area (m^2 kg^{-1})	443	342	440	419	371	390
Initial set (20 °C) (min)	125	160	15	15	10	10
Final set (20 °C) (min)	205	245	20	20	15	20

Table 3
Physicomechanical properties and total porosity of mortars after 90-day curing

Property of the mortar	Type of cement mortar cured in dry (D) and wet (W) air					
	MPC	MBFSPC	MSAB 1	MB (1)	MSAB 2	MB (2)
Compressive strength (MPa) (D)	52.1	35.1	5.8	20.6	6.4	18.7
Compressive strength (MPa) (W)	66.2	40.2	12.8	32.0	12.8	26.9
Absorption capacity (wt.%) (W)	7.1	8.0	10.7	8.4	10.9	9.4
Specific gravity (kg m^{-3}) (W)	2636	2678	2796	2714	2808	2771
Bulk density (kg m^{-3}) (W)	2286	2274	2159	2253	2148	2232
Total porosity (vol.%) (W)	13.3	15.1	22.8	17.0	23.5	19.5

(D): 20 °C/60% RH–dry air cure.
(W): 20 °C/100% RH–wet air cure.

The length changes of prisms were measured by a portable mechanical strain gauge apparatus (in a glass tube to minimize extraneous effects). The gauge length was 100 mm, with a measuring accuracy of 0.001 mm. Changes in length of mortar specimens are expressed in per mille (‰). The relation of per mille to microstrain is 1 μs = 0.001‰. The pH values of mortar extracts were determined by a pX meter OP 113 (Radelkis, Hungary). Potentiodynamic curves of steel bars were obtained using a Potentiostat OH 405 (Radelkis) at a polarization rate of 30 mV min^{-1}. Steel bars with diameter of 6 mm were immersed in mortar extract to determine the corrosion state.

Powder X-ray diffraction patterns were recorded on a Philips X-ray diffractometer coupled with an automatic data recording system. CuK$_\alpha$ radiation and Ni-filter were used. The chemical composition of the mortars was estimated by analytical methods. The oxide content in the soluble portion relating to the cement binder in weight percent was calculated. Simultaneous thermogravimetry (TG) and differential thermal analysis (DTA) were conducted from 20 to 1000 °C using a T.A.I. SDT 2960 Instrument (sample mass 10–20 mg, heating rate 10 °C/min, in flowing air). The pore structure was represented by the mercury porosimetry test using the high-pressure porosimeter model 2000 and macroporosimetry unit 120 (both Carlo Erba, Italy). The following pore structure characteristics were estimated: volume of micropores (to 7500 nm); micropore and pore median radius and porosity ranged between pore radius 3.75 nm and 0.2 mm.

3. Results and discussion

3.1. Mechanical properties and steel passivation

Six types of mortar specimens—the mortar with 100 wt.% of PC (indicated in the text as MPC), 100 wt.% of BFSPC (MBFSPC), 100 wt.% of SAB 1 cement (MSAB 1), 100 wt.% of SAB 2 cement (MSAB 2) as well as the mortar with a blend of 85 wt.% of SAB 1 cement/15 wt.% of PC [indicated in the text as MB (1)] and the mortar with a blend of 85 wt.% of SAB 2 cement/15 wt.% of PC [MB (2)]—were used in the experiments. Compressive strength, water

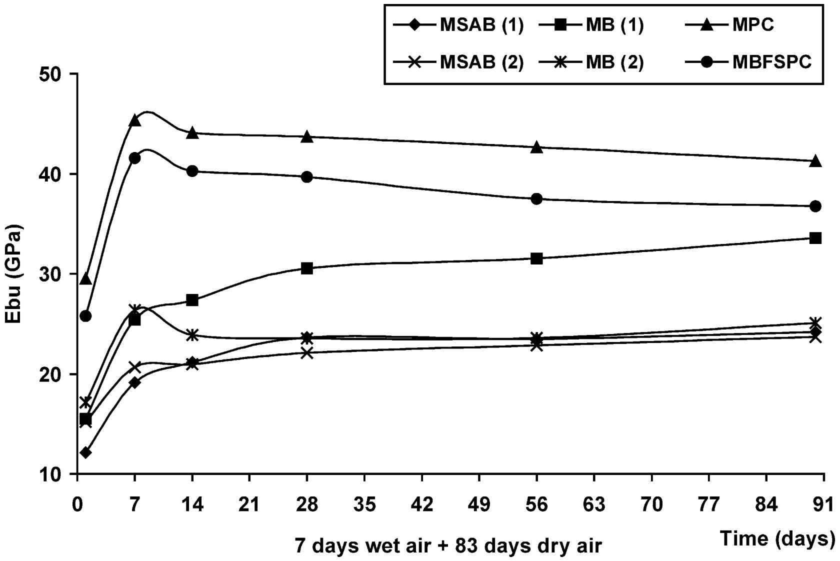

Fig. 1. Changes in dynamic modulus of elasticity (E_{bu}) of test mortars kept in 20 °C/60% RH–dry air.

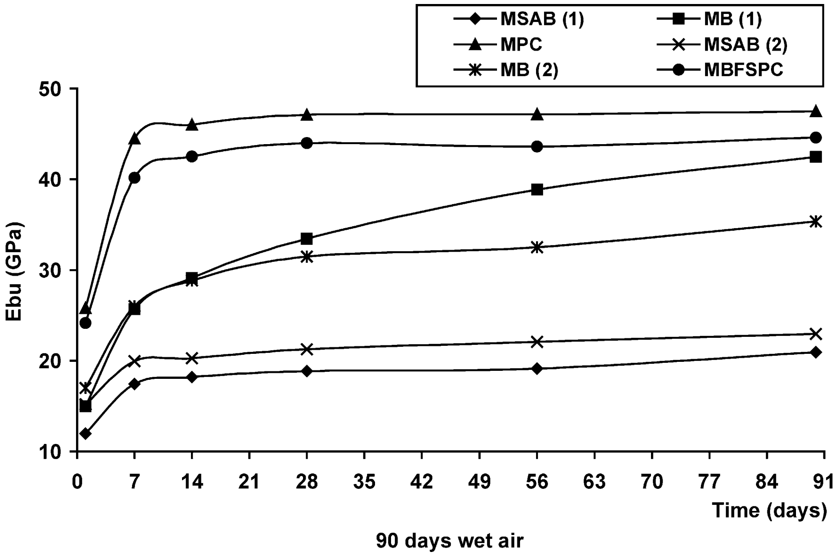

Fig. 2. Changes in dynamic modulus of elasticity (E_{bu}) of test mortars kept in 20 °C/100% RH–wet air.

absorption capacity and total porosity of mortars were considerably influenced by the type of cement and curing conditions. Experimental data indicated that the blending of SAB cement with PC is a possible way to upgrade the properties of SAB cement (Table 3, Figs. 1 and 2). The shrinkage compensation properties of SAB cements are evident from Fig. 3. The difference in 90-day values of length changes between specimens with SAB cements and other samples is approximately 0.60‰. This is in good agreement with English and Chinese experience of calcium sulfoaluminate cements in practice [24–27]. PC mortar and MB (1) as well as MSAB 2 cement mortar show a slight shrinkage under moist air cure (Fig. 4). BFSPC mortar and MB (2) as well as MSAB 1 cement mortar tend to expand a little. Differences in 90-day length changes of mortars kept in moist air cure are only ca. 0.20‰. The results given in Table 3 and Figs. 1, 2, 3 and 4 offer a real picture of the dependence between the cement mortar composition and important engineering properties.

Fig. 5a shows potentiodynamic curves of steel in PC and BFSPC mortar extracts and related pH values. Both curves are characterized by a long passive zone with a constant current density over a wide range of potentials. This confirms the passive state of steel in these mortars. The potentiodynamic curves of steel in the extracts of SAB cement mortars (pH = 10.23 and 10.53) have an entirely different course. The steel is depassivated (Fig. 5b). The addition of 15 wt.% of PC to SAB cement in test mortars [MB (1) and MB (2)] provides a complete passivation of steel comparable to those of PC and BFSPC mortars. The increased pH values of the mortar extracts (12.10 and 12.40) are evidence in support of this statement.

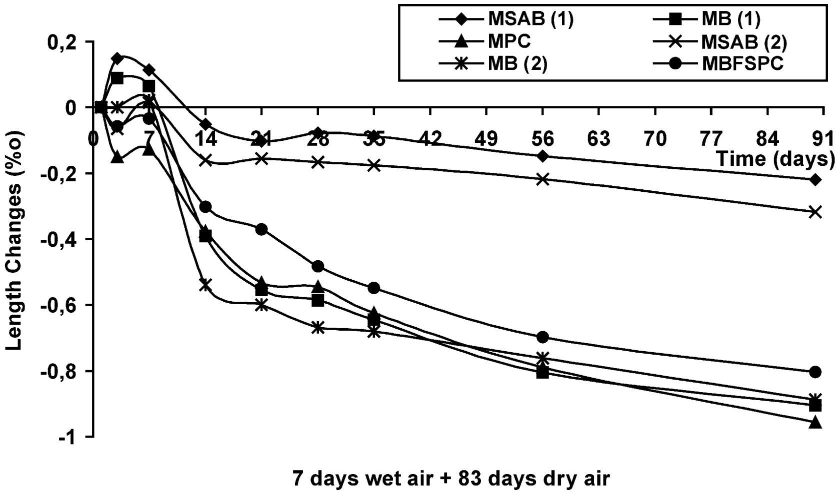

Fig. 3. Development in length changes of the mortars cured in 20 °C/60% RH–dry air.

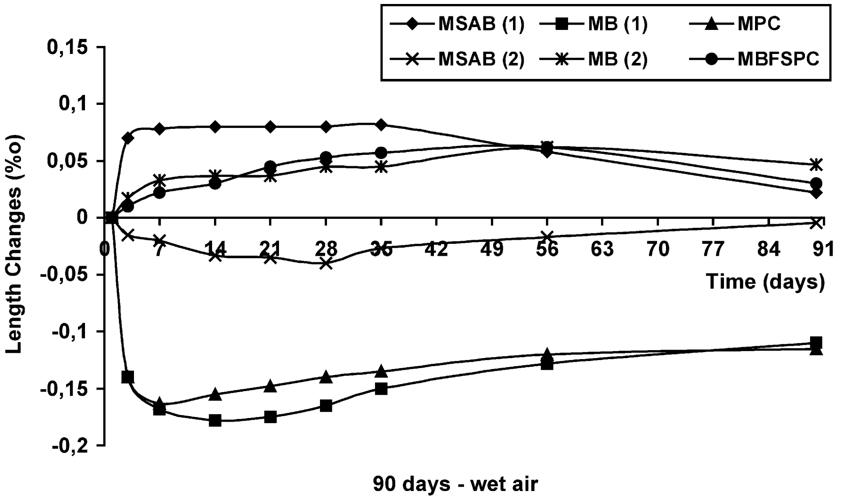

Fig. 4. Development in length changes of the mortars cured in 20 °C/100% RH–wet air.

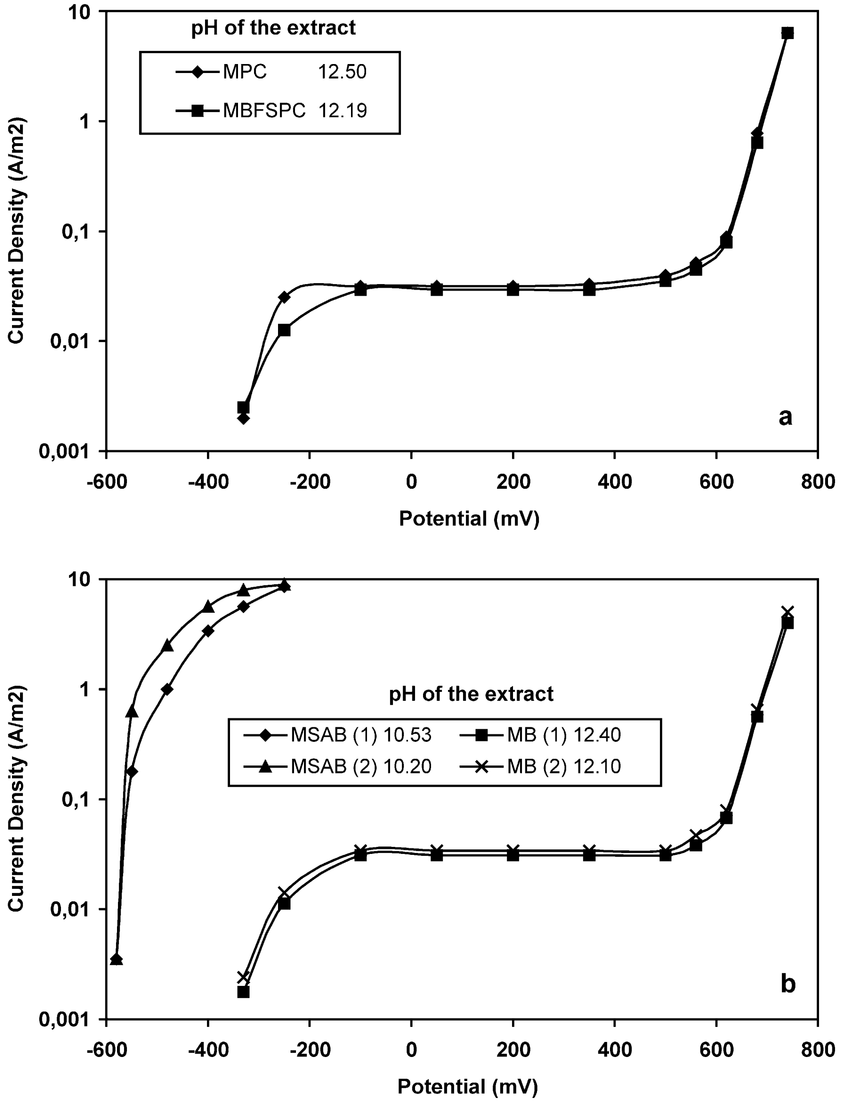

Fig. 5. Potentiodynamic curves of steel in mortars extracts after 90 days of wet curing.

The results have been interpreted to indicate increased strength and elasticity modulus on the one hand and decreased water absorption capacity and total porosity on the other hand of mortars made with the above blends relative to pure SAB cement mortars. SAB cement mortars have reduced shrinkage relative to PC mortar. Passivation of steel in SAB/PC mortars with 15 wt.% of PC is comparable to that in the pure PC and BFSPC mortar.

The qualitative disadvantage of SAB cements has to be removed by better raw material composition (the choice and mutual ratios) for SAB cement preparation. Significant improvements in utility properties of SAB/PC blends can then be expected.

The above data show that manufacture of relatively cheap cements that are environmentally acceptable both in their production and use (SAB cements and their blends with PC) is potentially very important. The SAB cement production is of great advantage from the viewpoint of energy savings and reduction of CO_2 quantity released into the atmosphere.

3.2. Cement hydration and pore structure

It is clear that the mechanical properties of mortars are considerably influenced by microstructure development through changes induced during cement hydration and hardening of the bonding system in the cement paste under the given curing conditions.

The chemical composition of test mortars kept for 90 days in moist air cure is given in Table 4. The CaO content in the soluble portion of SAB and SAB/PC cement mortars has decreased relative to that of PC mortar. However, higher contents of Fe_2O_3, Al_2O_3 and SO_3 are found in SAB and SAB/PC mortars compared to PC mortar.

Table 4
Chemical composition of mortars cured 90 days in 20 °C/100% RH–wet air

Mortar		$SiO_{2,S}$	CaO	Fe_2O_3	Al_2O_3	MgO	SO_3
MPC	5.18[a]						
	22.67[b]	4.96[c]	14.42[c]	0.73[c]	1.66[c]	0.20[c]	0.70[c]
	70.60[d]	21.88[e]	63.61[e]	3.22[e]	7.32[e]	0.88[e]	3.09[e]
MBFSPC	4.55[a]						
	21.34[b]	5.24[c]	11.14[c]	1.58[c]	1.97[c]	0.78[c]	0.63[c]
	72.82[d]	24.56[e]	52.20[e]	7.40[e]	9.23[e]	3.66[e]	2.95[e]
MSAB 1	2.18[a]						
	22.57[b]	4.80[c]	12.80[c]	1.65[c]	1.92[c]	0.28[c]	1.12[c]
	74.35[d]	21.27[e]	56.71[e]	7.31[e]	8.51[e]	1.24[e]	4.96[e]
MB (1)	4.54[a]						
	22.61[b]	4.77[c]	13.28[c]	1.39[c]	1.97[c]	0.15[c]	1.05[c]
	71.18[d]	21.10[e]	58.74[e]	6.15[e]	8.71[e]	0.66[e]	4.64[e]
MSAB 2	2.48[a]						
	21.72[b]	4.63[c]	12.35[c]	1.59[c]	1.97[c]	0.10[c]	1.08[c]
	74.86[d]	21.32[e]	56.86[e]	7.32[e]	9.07[e]	0.46[e]	4.97[e]
MB (2)	3.03[a]						
	20.99[b]	4.40[c]	12.39[c]	1.05[c]	2.15[c]	0.10[c]	0.90[c]
	74.56[d]	20.96[e]	59.03[e]	5.00[e]	10.24[e]	0.48[e]	4.29[e]

[a] Ignition loss (wt.%).

[b] Soluble portion (wt.%).

[c] Composition of soluble portion (wt.%).

[d] Insoluble portion (wt.%).

[e] Oxide content related to cement binder (wt.%).

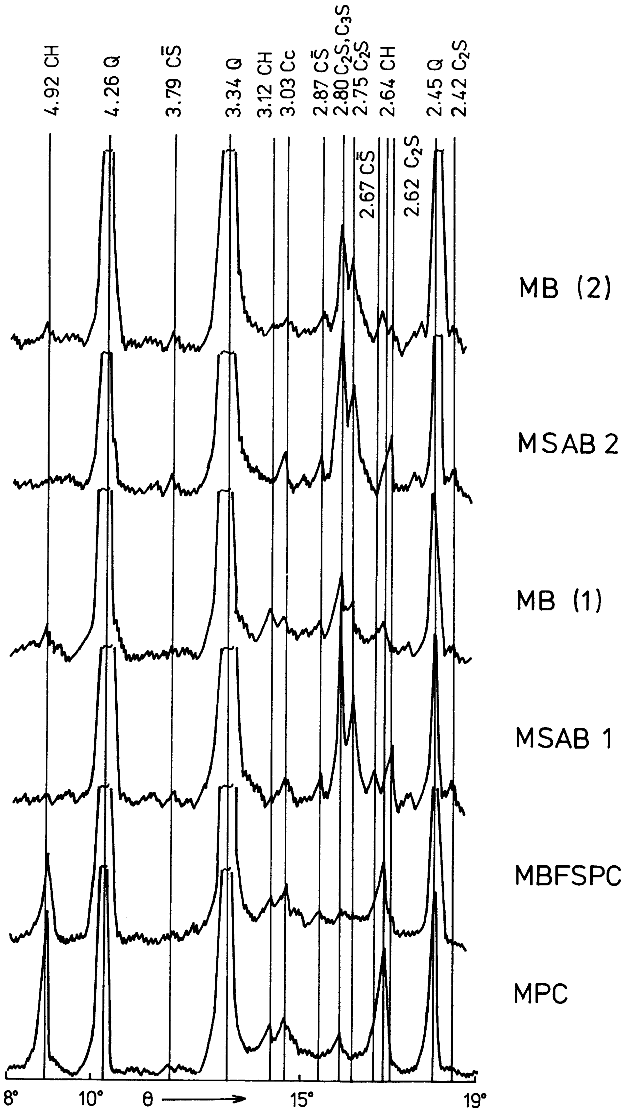

Fig. 6. X-ray diffractograms of test mortars after 90-day wet air cure.

The character of changes in strength, elasticity modulus, total porosity and shrinkage/expansion behavior is influenced mainly by the hydrate phase and pore structure development. Results of X-ray diffraction analysis of test mortars are shown in Fig. 6. The $Ca(OH)_2$ diffraction peaks (4.92 and 2.64 Å) are clearly seen in the PC and BFSPC mortars, and even in MB (1) and MB (2), the mortars incorporating 15 wt.% addition of PC. Ettringite was not detected, presumably due to the low $C_4A_3\bar{S}$ content. Conversion of unreacted belite or alite is characterized by the doublet in the region of 2.78 and 2.74 Å, which generally corresponds to these two clinker minerals. Both SAB cement mortars exhibit considerably decreased conversion of unreacted belite to hydration products. Its conversion in

MB (1) and MB (2) mortars is evident; and in BFSPC and PC mortars is markedly accelerated.

Thermal decomposition of the samples was studied by means of TG and DTA. Thermoanalytical data of the samples are summarized in Table 5. Generally, four significant temperature regions for all types of samples are observed:

1. Up to 400 °C—main temperature region of decomposition of the cement hydration products (CSH, $C\bar{S}H_2$, AFt and AFm phases). The interpretation of the thermogravimetric curves in this region was made more difficult because the range of decomposition temperatures of CSH, ettringite, gypsum and AFm phases lie close together [28–31].
2. 400–550 °C—temperature region of $Ca(OH)_2$ decomposition [28–30].
3. 550–800 °C—temperature region of carbonate, hydrated aluminate and the final stage of CSH phase decomposition [28–31].
4. Above 800 °C—temperature region of recrystallization of new nonbinding phases arising from hydrated cement minerals under recombustion [32].

However, small differences in the temperature ranges for the different samples were observed which are presented in Table 5.

The observed bound water loss in MB (1) and MB (2) mortars and the mainly PC mortar, and $Ca(OH)_2$ dehydroxylation in PC, BFSPC and partially in MB (1) mortar clearly confirm previous results of X-ray diffraction analysis. Both SAB cements are insufficiently reactive to offer such a degree of hydration giving strength and elasticity characteristics of mortars comparable to PC and BFSPC mortar. The 15 wt.% addition of PC to SAB cement improves significantly the hydrate phase formation relative to the pure SAB cement, but not to such an extent as to be comparable with hydrate phase development in PC or BFSPC mortar. The qualitative improvement of SAB cements is urgently required to be competitive with BFSPC. To achieve it, SAB cements with the mainly increased $C_4A_3\bar{S}/C_4AF$ and $C_4A_3\bar{S}/C\bar{S}$ ratios are suggested.

Table 5
Summary of TG intervals (°C) and DTA peak temperatures (°C) of the samples

Sample	TG	DTA	
PC	20–400 (CSH, $C\bar{S}H_2$, AFt, AFm)	71, 148	Endo
	400–550 (CH)	433	Endo
	550–800 (Q, $C\bar{C}$)	570	Endo
	Above 800 (recrystallization)	904	Exo
BFSPC	20–400 (CSH, $C\bar{S}H_2$, AFt, AFm)	31, 73	Endo
	400–550 (CH)	435	Endo
	550–800 (Q, $C\bar{C}$)	571	Endo
	Above 800 (recrystallization)	899	Exo
SAB 1	20–350 (CSH, $C\bar{S}H_2$, AFt, AFm)	68, 229	Endo
	350–550 (CH)	416	Endo
	550–800 (Q, $C\bar{C}$)	574	Endo
	Above 800 (recrystallization)	897	Exo
SAB 1 + PC (85 + 15)	20–250 (CSH, $C\bar{S}H_2$, AFt, AFm)	71	Endo
	250–525 (CH)	430	Endo
	525–800 (Q, $C\bar{C}$)	571	Endo
	Above 800 (recrystallization)	897	Exo
SAB 2	20–450 (CSH, $C\bar{S}H_2$, AFt, AFm)	66, 197	Endo
	450–580 (CH)	409	Endo
	580–785 (Q, $C\bar{C}$)	574	Endo
	Above 785 (recrystallization)	898	Exo
SAB 2 + PC (85 + 15)	20–340 (CSH, $C\bar{S}H_2$, AFt, AFm)	66, 146	Endo
	340–500 (CH)	367	Endo
	500–800 (Q, $C\bar{C}$)	571	Endo
	Above 800 (recrystallization)	902	Exo

Table 6
Pore structure of mortar specimens cured 90 days in 100% RH–wet air

Type of mortar	Micropore volume up to 7500 nm (%)	Micropore	Pore	Porosity (3.75 nm–0.2 mm) (%)
		median radius		
		(nm)	(nm)	
MPC	95.4	52.0	53.7	11.3
MBFSPC	89.2	55.9	62.1	13.9
MSAB 1	97.5	255.6	263.7	22.0
MB (1)	90.5	55.8	56.9	15.9
MSAB 2	91.5	276.5	304.4	23.0
MB (2)	94.1	45.3	47.2	17.4

The drop in the hydrate phase volume in SAB cement mortars induces a micropore and pore median radius and porosity increase (Table 6) compared to PC and BFSPC mortars. However, the pore structure characteristics of mortars with mixed cements [MB (1) and MB (2)] indicate distinct similarities with those made from PC and BFSPC. The positive role of PC in the blend with SAB cement is evident. Data given in Tables 6 and 7 undoubtedly confirm the phenomenon of pore structure "coarsening" due to SAB cement use in the mortar. The increase in porosity is due to a higher proportion of micropores with a radius of 100–500 nm within the SAB cement mortar structure relative to PC and BFSPC mortars with the decisive percentage of micropores between a radius of 3.75 and 100 nm. The pore size distribution of MB (1) and MB (2) mortars is similar to that of PC and BFSPC mortars. The 15 wt.% of PC portion in the blend with SAB cement is enough to make possible qualitative improvements in pore structure and pore size distribution of the observed mortars in comparison with pure SAB cement mortar. The pore structure characteristics of MB (1) and MB (2) mortars are similar to those of PC

Table 7
Pore size distribution of mortars after 90-day wet air cure

Type of mortar	Pores portion (%)					
	3.75–50 nm	50–100 nm	100–500 nm	500–1000 nm	1000–7500 nm	over 7500 nm
MPC	40.4	44.3	5.9	3.0	3.4	3.0
MBFSPC	37.0	30.6	10.5	3.2	7.3	11.4
MSAB 1	17.2	7.8	57.0	11.0	4.9	2.1
MB (1)	34.5	48.3	2.0	2.1	4.1	9.0
MSAB 2	16.5	11.7	52.6	6.1	4.7	8.4
MB (2)	48.0	29.3	11.8	0.7	5.0	5.2

and BFSPC mortars. This confirms the positive influence of the PC portion in blends made with the SAB cements.

Strength and elasticity characteristics, deformation behavior and passivation ability of the mortars vary, depending on the type of cement or cement blend used in the mortar. Different types of hydration products and hydration degree in the studied mortars form pore structures with diverse and markedly characteristic pore size distribution. The utility properties of SAB cement mortars are considerably improved by 15 wt.% replacement of SAB cement by PC. The reasons for this fact are the increase in volume of the hydrate phase and $Ca(OH)_2$; and the formation of finer pore structure in the mortar with a mixed cement. In SAB/PC mortar, sufficient alkalinity for complete protection of steel against corrosion is provided.

4. Conclusions

The following conclusions are applicable to the particular mortars and test conditions employed:

1. The replacement of 15 wt.% SAB cement by PC offers a blend suitable for mortar preparation with increased strength and elasticity modulus as well as decreased water absorption capacity and total porosity compared to the pure SAB cement mortar.
2. The reason for this fact are differences in the crystal structure and microstructure of the hydrate phase that develops, pore structure and percentage portion of individual pores of distinct pore radii.
3. Passivation of steel in the mortar with a blend of 85 wt.% of SAB cement and 15 wt.% of PC is comparable to that in pure PC and BFSPC mortar. Steel is depassivated in pure SAB cement mortars.
4. The improvement in SAB cement quality is unavoidably required to be competitive with at least BFSPC in mortar and concrete-making technological procedures in the future.

Acknowledgements

The authors wish to thank the Slovak Grant Agency VEGA (project no. 2/7035/21) for the financial support.

References

[1] P.K. Mehta, Investigation on energy saving cement, World Cem. Technol. 11 (4) (1991) 166–177.

[2] W. Jiang, M.R. Silsbee, D.M. Roy, Similarities and differences of microstructures and macroproperties between portland and blended cement, Cem. Concr. Res. 27 (10) (1997) 1501–1511.

[3] I. Odler, H. Zhang, Investigations on high SO_3 portland clinkers and cements: I. Clinker synthesis and cement preparation, Cem. Concr. Res. 26 (9) (1996) 1307–1313.

[4] H. Zhang, I. Odler, Investigations on high SO_3 portland clinkers and cements: II. Properties of cements, Cem. Concr. Res. 26 (9) (1996) 1315–1324.

[5] J.H. Sharp, C.D. Lawrence, R. Yang, Calcium sulfoaluminate cements—low-energy cements, special cements or what? Adv. Cem. Res. 11 (1) (1999) 3–13.

[6] I. Beretka, L. Santoro, N. Sherman, G.L. Valenti, Synthesis and properties of low energy cements based on $C_4A_3\bar{S}$, Proc. 9th Int. Congr. Chem. Cem., New Delhi, Vol. III, Theme II, A. K. Mullick, National Council for Cement and Building Materials, New Delhi, 1992, pp. 195–200.

[7] M. Ali, S. Gopal, S.K. Handoo, Studies on the formation kinetics of calcium sulfo-aluminate, Cem. Concr. Res. 24 (4) (1994) 715–720.

[8] G.K. Moir, F.P. Glasser, Mineralisers, modifiers and activators in the clinkering process, Proc. 9th Int. Congr. Chem. Cem., New Delhi 1 (1992) 125–152.

[9] M. Su, Y. Wang, L. Zhang, D. Li, Preliminary study on the durability of sulfo/ferro-aluminate cements, Proc. 10th Int. Congr. Chem. Cem., Gothenburg 4 (1997) 4iv029.

[10] Y. Wang, S. Li, M. Su, J. Xu, F. Zhang, Sulpho-aluminate cement with low alkalinity, Proc. 10th Int. Congr. Chem. Cem., Gothenburg 4 (1997) 4iv030.

[11] S.A. Brooks, J.H. Sharp, in: R.I. Mangabhai, F.N. Spon (Eds.), Ettringite-Based Cements, Calcium Aluminate Cements, F&N Spon, London, 1990, pp. 1–335.

[12] J. Majling, S. Sahu, M. Vlna, D.M. Roy, Relationship between raw mixture and mineralogical composition of sulphoaluminate belite clinkers in the system $CaO-SiO_2-Al_2O_3-Fe_2O_3-SO_3$, Cem. Concr. Res. 23 (6) (1993) 1351–1356.

[13] J. Strigáč, J. Krištin, S. Sahu, M.T. Palou, J. Majling, An approach to refine the Bogue's phase composition of sulphoaluminate belite cement, Proc. 10th Int. Congr. Chem. Cem., Gothenburg 3 (1997) 3v009.

[14] P. Arjunan, M.R. Silsbee, D.M. Roy, Sulfoaluminate-belite cement from low-calcium fly ash and sulfur-rich and other industrial by-products, Cem. Concr. Res. 29 (6) (1999) 1305–1311.

[15] J. Beretka, M. Marroccoli, N. Sherman, G.L. Valenti, The influence of $C_4A_3\bar{S}$ content and w/s ratio on the performance of calcium sulfoaluminate-based cements, Cem. Concr. Res. 26 (11) (1996) 1673–1681.

[16] J. Strigáč, M.T. Palou, J. Krištin, J. Majling, Morphology and chemical composition on minerals inside the phase assemblage $C-C_2S-C_4A_3\bar{S}-C_4AF-C\bar{S}$ relevant to sulphoaluminate belite cements, Ceram.-Silik. 44 (1) (2000) 26–34.

[17] J. Beretka, B. de Vito, L. Santoro, N. Sherman, G.L. Valenti, Hydraulic behaviour of calcium sulfoaluminate-based cements derived from industrial process wastes, Cem. Concr. Res. 23 (5) (1993) 1205–1214.

[18] N. Sherman, J. Beretka, L. Santoro, G.L. Valenti, Long-term behaviour of hydraulic binders based on calcium sulfoaluminate and calcium sulfosilicate, Cem. Concr. Res. 25 (1) (1995) 113–126.

[19] V. Živica, I. Janotka, Chemical resistance of sulfoaluminate-belite cement-based materials, Build. Res. J. 47 (2) (1999) 117–134.

[20] I. Janotka, L'. Krajči, Resistance to freezing and thawing of mortar specimens made from sulphoaluminate-belite cement, Bull. Mater. Sci. 23 (6) (2000) 521–527.

[21] S.C. Mojumdar, Processing-moisture resistance and thermal analysis of MDF materials, J. Therm. Anal. Calorim. 64 (2001) 1133–1139.

[22] M. Drabik, L. Galikova, F. Hanic, J.H. Sharp, MDF-related compositions based on novel low-energy clinker, Chem. Pap. 51 (1997) 363–366.

[23] I. Janotka, L'. Krajči, An experimental study on the upgrade of sulfoaluminate-belite cement systems by blending with portland cement, Adv. Cem. Res. 11 (1) (1999) 35–41.

[24] L. Zhang, M. Su, Y. Wang, New developments in the use of sulfoaluminates and sulfoferro-aluminate cements in China, Proc. Conf. Cements for the Future—Calcium Sulpho-aluminates, London, Session 2, Book of Abstracts, F. P. Glasser, The Institute of Materials and Society of Chemical Industry, London, 1998.

[25] A.D.R. Brown, Commercial, production, composition and properties of a calcium sulfoaluminate cement, Proc. Conf. on Cements for the

Future—Calcium Sulphoaluminates, London, Session 3, Book of Abstracts, F. P. Glasser, The Institute of Materials and Society of Chemical Industry, London, 1998.

[26] R.F. Viles, Some commercial applications of calcium sulphoaluminate cements in construction and mining, Proc. Conf. on Cements for the Future—Calcium Sulphoaluminates, London, Session 4, Book of Abstracts, F. P. Glasser, The Institute of Materials and Society of Chemical Industry, London, 1998.

[27] D. Johnson, Use of calcium sulfoaluminate cements in the construction industry, Proc. Conf. on Cements for the Future—Calcium Sulphoaluminates, London, Session 4, Book of Abstracts, F. P. Glasser, The Institute of Materials and Society of Chemical Industry, London, 1998.

[28] H.F.W. Taylor, Cement Chemistry, 2nd ed., Thomas Telford Publ., London, 1998.

[29] C.D. Lawrence, in: P.C. Hewlett (Ed.), Lea's Chemistry of Cement and Concrete Chapter 9: The Production of Low Energy Cements, 4th ed., Edward Arnold Publ., London, 1998, pp. 421–470.

[30] M. Drabik, S.C. Mojumdar, L. Galikova, Changes of thermal events of macro-defect-free (MDF) cements due to the environmental deterioration, Cem. Concr. Res. 31 (5) (2001) 743–747.

[31] C.A. Strydom, J.H. Potgieter, An investigation into the chemical nature of the reactivity of lime, Proc. 10th Int Congr. Chem., Gothenburg 2 (1997) 2ii049.

[32] I. Janotka, T. Nürnbergerová, L. Nad, Behaviour of high-strength concrete with dolomitic aggregate at high temperatures, Mag. Concr. Res. 52 (6) (2000) 399–409.